

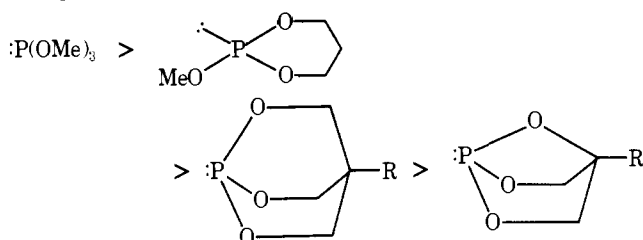
Phosphorus Ester Basicity Dependence on Constraint. Crystal and Molecular Structures of $P(OCH_2)_3CCH_2Br$ and $O=P(OCH_2)_2C(CH_3)O$

D. S. Milbrath, J. P. Springer, J. C. Clardy,¹ and J. G. Verkade*

Contribution from Gilman Hall and the Ames Laboratory—ERDA, Iowa State University, Ames, Iowa 50011. Received December 11, 1975

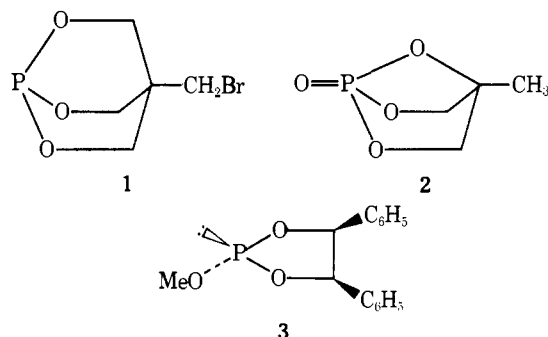
Abstract: Structural parameters of the title compounds along with those of similar systems reported earlier can be related by means of hybridization considerations to the decrease in basicity of phosphorus realized upon constraint of the alkoxy groups. It is concluded that the $:P(OCH_2)_3CR$ cage is essentially unstrained but that oxidation to $O=P(OCH_2)_3CR$ induces stress primarily in the POC angles. In $O=P(OCH_2)_2C(CH_3)O$ (**2**), however, compression of both the OPO and POC angles is observed. The unit cells were found to be orthorhombic, $P_{2_12_12_1}$, $a = 5.823$ (1), $b = 7.956$ (1), and $c = 16.695$ (2) Å, and $Pnma$, $a = 8.928$ (1), $b = 8.148$ (1), and $c = 8.410$ (1) Å, for $P(OCH_2)_3CCH_2Br$ and **2**, respectively. Final R factors using anisotropic temperature factors with inclusion of the hydrogen positions are 0.036 and 0.028 for 602 and 379 reflections, respectively, measured on a Syntex P2₁ diffractometer.

The decreasing Lewis basicity of the trivalent phosphorus lone pair in the series



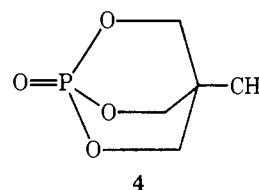
has been established from studies of the trends in BH_3 adduct equilibria,² $^1J_{PH}$ values of the protonated forms,³ BH stretching frequencies of the BH_3 adducts,⁴ and the CO^5 and NO^6 stretching modes of their transition metal complexes. While this basicity trend is somewhat surprising in view of the decreasing steric encumbrance experienced by a BH_3 group or a transition metal upon coordination of these bases, the results can be accounted for in terms of a "hinge effect"⁷ and orbital symmetry arguments⁸ (vide infra).

Germane to the problem of the basicity decrease upon molecular constraint, as well as the unusually high toxicity of $P(OCH_2)_3CR$,⁹ is the question of increased strain in a caged phosphorus ester. We therefore undertook the molecular structure determination of **1** and **2**. In contrast to the relative



ease in obtaining solid state structural analyses for pentavalent phosphorus esters, trivalent phosphorus esters tend to be low-melting substances which turn into glasses on cooling or they are reluctant to form suitable crystals. The x-ray structure determination of **3** which appeared recently¹⁰ constitutes the first such structural report on this class of compounds. Electron diffraction experiments on triethyl and trivinyl phosphite¹¹ produced bond angle data too crude for purposes of comparison.

In this paper it is shown from the structural data that **1** appears to be quite strainless but that polarization of the phosphorus lone pair as in **4** induces strain primarily by bending of the POC angles. The structural parameters of **2** further confirm the operation of such a "hinge effect"⁷ in polycyclic phosphorus triester systems and also show that the additional stress imposed by a one-atom bridge in this molecule forces phosphorus to rehybridize appreciably in contrast to **4**.



Experimental Section

Preparation of 1. In a 250-ml round-bottom flask were reacted 5.0 g (0.025 mol) of $BrCH_2C(CH_2OH)_3$ ¹² and 3.2 g (0.026 mol) of trimethyl phosphite under conditions described previously.¹³ A 69% yield of product (mp 80–82 °C) was isolated by sublimation at 50° and 0.1 mm of pressure. The proton NMR spectrum in $CDCl_3$ (δ_{CH_2} 4.07 d (3), $^3J_{PH} = 3$ Hz; δ_{CH_2} 3.01 s (1)) and proton decoupled $\delta^{31}P$ (–91.8 ppm downfield from external 85% H_3PO_4) were consistent with a bicyclic structure. Parent ion peaks in the correct isotopic ratio were observed at m/e 226 and 228 in the mass spectrum.

Preparation of 2. This compound was prepared as has been previously reported.^{3b}

Data Collection. Crystals of **1** were grown by sublimation onto a water-cooled probe at 40–50° and 0.1 mm. A columnar crystal, 0.13 × 0.28 × 0.35 mm, was selected for data collection and mounted in a Lindeman capillary to protect it from atmospheric moisture.

Suitable crystals of **2** were obtained from a methylene chloride solution to which ethyl ether was added to the cloud point followed by cooling to –78 °C overnight. From the soft needles formed, a fragment, 0.12 × 0.22 × 0.51 mm, was mounted in a Lindeman capillary to eliminate hydrolysis from atmospheric moisture.

Data from both crystals were taken using a Syntex P2₁ automated four-circle diffractometer operating with graphite monochromated $Cu K\alpha$ radiation (λ 1.5418 Å). Preliminary examination of the crystals showed them both to be orthorhombic with unit cells, **1**, $a = 5.823$ (1), $b = 7.956$ (1), and $c = 16.695$ (2) Å, and **2**, $a = 8.928$ (1), $b = 8.148$ (1), and $c = 8.410$ (1) Å.

A measured density for crystals of **2** of 1.62 g/ml agrees well with a density of 1.629 g/ml calculated on the basis of four molecules per unit cell. No satisfactory medium was found for the density measurement of **1** owing to its high degree of solubility.

A variable ω -scan technique (1.0°/min minimum scan speed) was employed to measure 661 reflection intensities of **1** within a 2θ sphere of 114.1° ($\sin \theta/\lambda = 0.544 \text{ \AA}^{-1}$). Of these reflections 602 were judged

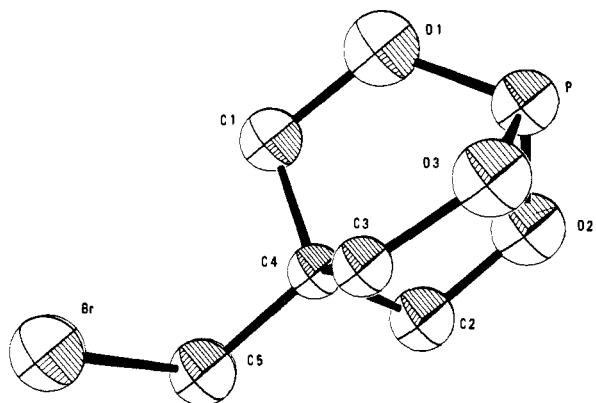


Figure 1. Computer drawing of the molecular structure of $\text{P}(\text{OCH}_2)_3\text{CCH}_2\text{Br}$ (**1**).

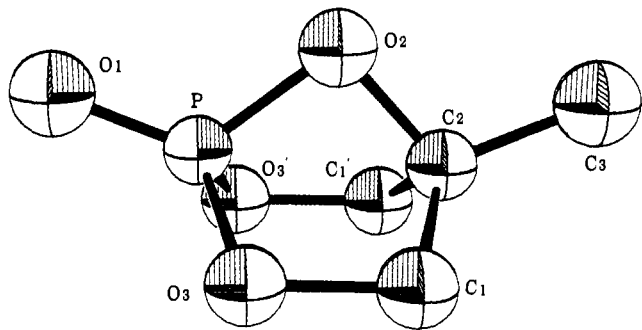


Figure 2. Computer drawing of the molecular structure of $\text{O}=\text{P}(\text{OCH}_2)_2\text{C}(\text{CH}_3)\text{O}$ (**2**).

to be observed after correction for Lorentz, polarization, and background effects ($F_o \geq 3\sigma(F_o)$). Systematic absences ($00l$, absent if $l = 2n + 1$; $0k0$, absent if $k = 2n + 1$; and $h00$, absent if $h = 2n + 1$) unambiguously identified the space group as $P2_12_12_1$.

Measurement of data from the crystal of **2** was carried out with a variable $2\theta/\theta$ -scan technique ($2.0^\circ/\text{min}$ minimum scan speed). After correction for Lorentz, polarization, and background effects, 379 reflections of 513 measured were judged observed ($F_o \geq 3\sigma(F_o)$). The space group was identified as $Pnma$ from the data extinctions ($0kl$, absent if $k + l = 2n + 1$ and $hk0$, absent if $h = 2n + 1$).

Solution and Refinement. Routine application of MULTAN as described by Germain et al.¹⁴ to data for **1** located the bromine and phosphorus positions. Least-squares refinement¹⁵ of these positions resulted in conventional weighted and unweighted discrepancy factors, R and R_w , of 0.287 and 0.304. From the phosphorus-bromine phased electron density calculations,¹⁶ the positions of the remaining non-hydrogen atoms were located and refined to $R = 0.119$ and $R_w = 0.146$. Isotropic refinement of positional and temperature factors did not change the agreement factors greatly ($R = 0.112$ and $R_w = 0.136$) but anisotropic treatment of the model resulted in $R = 0.046$ and $R_w = 0.042$. A Fourier-synthesis difference calculation¹⁶ allowed all of the hydrogen atom positions to be found. Final refinement of all positions and temperature coefficients produced $R = 0.036$ and $R_w = 0.032$.

Solution of the structure of **2** was also begun with the use of MULTAN. The phosphorus position was found from the solution and was refined by least-squares methods to $R = 0.546$ and $R_w = 0.563$. All of the non-hydrogen atoms were easily located in the phased electron-density calculation. Refinement resulted in agreement factors of 0.165 and 0.197 for R and R_w , respectively. Subsequent refinement with isotropic temperature factors ($R = 0.121$ and $R_w = 0.146$) followed by anisotropic temperature factors ($R = 0.056$ and $R_w = 0.058$) produced a difference Fourier synthesis from which all of the hydrogen atoms were located. Final refinement of the structure model resulted in agreement factors of $R = 0.028$ and $R_w = 0.028$.

Figures 1 and 2 show computer¹⁷ drawings of the molecular structures of **1** and **2**, respectively. The final positional and an isotropic temperature coefficients for these molecules are listed in Tables I and II, while their intramolecular bond distances and angles appear in Tables III and IV. The final observed and calculated structure factor amplitudes have been tabulated in the supplementary material.¹⁸ The atomic scattering factors used in these refinements were those of Hanson et al.¹⁹ Real and imaginary corrections for anomalous dispersion²⁰ for bromine and phosphorus were also used in the calculations.

Discussion

The average of the POC (117.5°) and OPO (100.1°) bond angles in **1** compare very favorably with the exocyclic POC angle (117.5°) and the average of the exocyclic OPO angles²¹ (100.8°) of **3**. Similarly, the averages of the CO (1.446 \AA) and PO (1.615 \AA) bond lengths of **1** are very close to those in **3** (1.449 and 1.623 \AA , respectively). These results are confirmatory of our earlier suggestion^{5a} that there is little if any strain in caged phosphite esters such as **1**.

Despite the lack of strain in **1**, the positive charge on the

Table I. Final Positional^a and Anisotropic Temperature^b Factors of $\text{P}(\text{OCH}_2)_3\text{CCH}_2\text{Br}$

Atom ^c	x	y	z	$\beta(1,1)^d$	$\beta(2,2)$	$\beta(3,3)$	$\beta(1,2)$	$\beta(1,3)$	$\beta(2,3)$
Br	0.1258 (1)	0.2980 (1)	0.4309 (1)	41.0 (3)	16.1 (1)	4.86 (3)	5.4 (2)	-1.36 (9)	2.18 (5)
P	-0.2797 (3)	0.8920 (2)	0.3634 (1)	37.5 (6)	10.6 (2)	3.45 (7)	3.5 (3)	0.3 (2)	0.3 (1)
O(1)	-0.3281 (9)	0.7849 (6)	0.4437 (2)	49.7 (21)	16.2 (8)	3.4 (2)	6.6 (11)	4.7 (5)	-0.1 (3)
O(2)	-0.4006 (11)	0.7740 (6)	0.2969 (3)	46.9 (22)	16.1 (8)	4.7 (2)	8.0 (12)	-5.5 (6)	0.1 (3)
O(3)	-0.0144 (9)	0.8428 (5)	0.3480 (3)	33.1 (16)	11.0 (8)	5.9 (2)	-2.5 (9)	2.0 (5)	1.6 (3)
C(1)	-0.2826 (12)	0.6062 (8)	0.4411 (4)	28.3 (20)	11.8 (9)	2.7 (2)	-1.7 (13)	1.1 (6)	0.5 (4)
C(2)	-0.3299 (14)	0.5989 (9)	0.2939 (4)	35.0 (29)	16.0 (12)	2.8 (2)	2.9 (16)	-2.0 (7)	-0.8 (4)
C(3)	0.0480 (11)	0.6681 (8)	0.3533 (4)	23.2 (19)	14.1 (11)	2.9 (2)	0.4 (11)	0.7 (6)	0.6 (4)
C(4)	-0.1664 (10)	0.5606 (7)	0.3634 (3)	21.7 (19)	10.9 (8)	2.2 (2)	-1.0 (11)	-0.9 (6)	-0.5 (3)
C(5)	-0.1138 (15)	0.3734 (8)	0.3581 (4)	34.5 (24)	12.4 (10)	3.7 (3)	2.0 (15)	-1.1 (8)	-0.9 (4)
H(1) ^e	-0.421 (12)	0.541 (8)	0.447 (3)	0.4 (12) ^f					
H(1A)	-0.189 (11)	0.583 (9)	0.489 (4)	1.2 (10)					
H(2)	-0.257 (13)	0.589 (11)	0.246 (6)	2.0 (15)					
H(2A)	-0.477 (21)	0.538 (13)	0.305 (6)	4.1 (23)					
H(3)	0.167 (12)	0.644 (8)	0.391 (4)	0.2 (10)					
H(3A)	0.114 (14)	0.645 (9)	0.304 (5)	1.5 (14)					
H(5)	-0.240 (20)	0.311 (16)	0.371 (6)	4.8 (24)					
H(5A)	-0.057 (14)	0.342 (10)	0.301 (5)	2.8 (17)					

^a Standard deviations are given in parentheses. ^b Anisotropic thermal ellipsoids are of the form $\exp[-(\beta_{11}h^2 + \beta_{22}k^2 + \beta_{33}l^2 + 2\beta_{12}hk + 2\beta_{13}hl + 2\beta_{23}kl)]$. ^c Numbering of the atoms corresponds to that in Figure 1. ^d All β values are $\beta \times 10^3$. ^e Hydrogen atoms are labeled with the number of the carbon atom to which they are bonded. Where more than one hydrogen is bonded to a carbon atom, the hydrogens are labeled with a number and a letter. ^f Hydrogen atom temperature factors are isotropic.

Table II. Final Positional^a and Anisotropic Temperature^b Factors of $\text{O}=\text{P}(\text{OCH}_2)_2\text{C}(\text{CH}_3)\text{O}$

Atom ^c	<i>x</i>	<i>y</i>	<i>z</i>	$\beta(1,1)^d$	$\beta(2,2)$	$\beta(3,3)$	$\beta(1,2)$	$\beta(1,3)$	$\beta(2,3)$
P	0.1196 (1)	0.7500	0.2403 (1)	13.7 (1)	12.8 (1)	7.5 (1)	0.0	0.11 (9)	0.0
O(1)	0.0596 (3)	0.7500	0.3998 (2)	18.7 (4)	23.7 (5)	9.8 (3)	0.0	2.4 (3)	0.0
O(2)	0.0140 (2)	0.7500	0.0875 (2)	12.9 (3)	18.0 (4)	10.3 (3)	0.0	-0.3 (2)	0.0
O(3)	0.2178 (2)	0.9036 (2)	0.1939 (1)	19.4 (3)	13.9 (3)	9.1 (2)	-2.6 (2)	-0.8 (2)	-1.2 (2)
C(1)	0.2249 (3)	0.9040 (3)	0.0183 (2)	17.4 (4)	13.5 (4)	8.7 (3)	-0.6 (3)	-0.2 (3)	1.4 (2)
C(2)	0.1388 (4)	0.7500	-0.0303 (3)	14.3 (4)	13.6 (5)	8.4 (4)	0.0	0.5 (4)	0.0
C(3)	0.0796 (5)	0.7500	-0.1975 (4)	19.2 (6)	18.4 (7)	9.9 (5)	0.0	-2.9 (4)	0.0
H(1) ^e	0.333 (3)	0.899 (3)	-0.015 (3)	2.4 (5) ^f					
H(1A)	0.176 (2)	1.004 (3)	-0.016 (2)	0.8 (4)					
H(3)	0.025 (3)	0.654 (4)	-0.214 (4)	3.4 (6)					
H(3A)	0.171 (6)	0.750	-0.277 (6)	4.5 (10)					

^a Standard deviations are given in parentheses. ^b The anisotropic thermal ellipsoid is of the form $\exp[-(\beta_{11}h^2 + \beta_{22}k^2 + \beta_{33}l^2 + 2\beta_{12}hk + 2\beta_{13}hl + 2\beta_{23}kl)]$. ^c Numbering of the atoms corresponds to that in Figure 2. ^d All β values are $\beta \times 10^3$. ^e Hydrogen atoms are labeled with the number of the carbon atom to which they are bonded. Where more than one hydrogen is bonded to a carbon atom the hydrogens are labeled with a number and a letter. ^f Hydrogen atom temperature factors are isotropic.

Table III. Intramolecular Bond Distances and Angles in $\text{P}(\text{OCH}_2)_3\text{CCH}_2\text{Br}^a$

Distance (Å)		Angles (deg)	
P-O(1)	1.613 (4)	O(1)-P-O(2)	100.8 (2)
P-O(2)	1.616 (5)	O(1)-P-O(3)	99.9 (2)
P-O(3)	1.615 (5)	O(2)-P-O(3)	99.6 (3)
O(1)-C(1)	1.446 (7)	P-O(1)-C(1)	117.6 (3)
O(2)-C(2)	1.454 (8)	P-O(2)-C(2)	117.2 (4)
O(3)-C(3)	1.440 (7)	P-O(3)-C(3)	117.7 (3)
C(1)-C(4)	1.509 (7)	O(1)-C(1)-C(4)	110.1 (4)
C(2)-C(4)	1.531 (8)	O(2)-C(2)-C(4)	109.9 (4)
C(3)-C(4)	1.522 (8)	O(3)-C(1)-C(4)	110.0 (4)
C(4)-C(5)	1.523 (8)	C(1)-C(4)-C(2)	109.0 (4)
C(5)-Br	1.945 (6)	C(1)-C(4)-C(3)	109.1 (4)
		C(2)-C(4)-C(3)	108.3 (4)
		C(1)-C(4)-C(5)	112.0 (4)
		C(2)-C(4)-C(5)	106.0 (4)
		C(3)-C(4)-C(5)	112.2 (5)
		C(4)-C(5)-Br	114.2 (4)

^a Numbering of atoms corresponds to Figure 1.

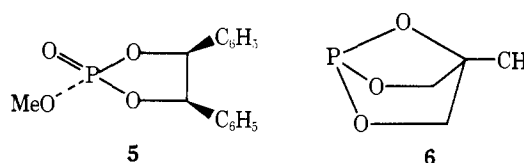
Table IV. Intramolecular Bond Distances and Angles in $\text{O}=\text{P}(\text{OCH}_2)_2\text{C}(\text{CH}_3)\text{O}^a$

Distance (Å)		Angle (deg)	
P-O(1)	1.445 (2)	O(1)-P-O(2)	121.9 (1)
P-O(2)	1.594 (2)	O(1)-P-O(3)	115.8 (1)
P-O(3)	1.577 (2)	O(2)-P-O(3)	97.4 (1)
O(3)-C(1)	1.478 (2)	O(3)-P-O(3)'	105.1 (1)
O(2)-C(2)	1.492 (4)	P-O(2)-C(2)	95.3 (2)
C(1)-C(2)	1.528 (3)	P-O(3)-C(1)	105.8 (1)
C(2)-C(3)	1.502 (4)	O(3)-C(1)-C(2)	104.1 (2)
		C(1)-C(2)-C(3)	115.3 (1)
		C(1)-C(2)-C(1)'	110.5 (3)
		O(2)-C(2)-C(3)	111.0 (3)
		O(2)-C(2)-C(1)	101.4 (2)

^a Numbering of the atoms corresponds to that in Figure 2. A prime (') denotes an atom generated by the mirror plane.

phosphorus has been calculated by the CNDO/2 method to be significantly higher than that of $\text{P}(\text{OMe})_3$ ^{3b} which is also strainless. This lends support to the proposal⁷ that the largely unhybridized p orbital on the essentially sp^2 oxygens is able to interact with the phosphorus lone pair in the acyclic phosphite because of the preferred conformational geometry of the POMe moieties, while in **1** these oxygen orbitals are orthogonal to the phosphorous lone pair owing to the symmetry imposed by the cage. While the reduction of the number of π donating interactions of these oxygen p orbitals to phosphorus d orbitals is also reduced for symmetry reasons,⁷ recent evidence from ab initio calculations suggests that this effect is negligible in trimethyl phosphate assuming tetrahedral oxygen and phosphorus configurations.²²

Upon polarization of the phosphorus lone pair by a Lewis acid, opening of the OPO angles and shortening of the PO bonds occurs as is clearly seen from **1** to **4**²⁴ (3.1° , 0.053 \AA) and from **3** to **5**¹⁰ (4.7° , 0.046 \AA). On the other hand, the unconstrained POC angle in the POCH_3 moiety of **3** and **5** remains



unchanged (117.5°) while it decreases from this value in **1** to 115.3° in **4**.²³ These data along with structural data for **2** suggest that the POC angle in four-coordinate phosphorus esters is more sensitive to constraint than the OPO angle. Thus in **2**, strain causes the average POC angle to contract from an unstrained angle of about 117° to 120° ⁷ in phosphate esters to 102° while the normal OPO angle of 104° in unstrained phosphates decreases to an average of 99.9° in **2**.

A consequence of the oxygen "hinge effect" is the progression from sp^2 toward sp^3 hybridization of this atom from $\text{O}=\text{P}(\text{OR})_3$ to **4** to **2** which could accentuate the accumulation of positive charge on phosphorus by partial destruction of π bonding in the three P—O ester links. This notion is consistent with the finding that caged phosphites exemplified by **1** and **6** behave as better π acids than acyclic phosphites toward transition metals,^{5a} presumably to compensate for the loss of π bonding from the caged ester oxygens.

Of note in the structure of **2** is the somewhat long P—O ester bond (1.59 \AA) and the short P=O link (1.445 \AA) compared to the averages of these distances in phosphate esters and acid phosphates (1.57 and 1.48 \AA , respectively).²⁴ It is reasonable

to suppose that the shortening of the phosphoryl bond stems from the relatively high degree of π bonding obliged to concentrate in this link owing to the geometrical restrictions to P—O π bonding imposed by the oxygen "hinge effect" and the strain-lengthened P—O bond.

Acknowledgments. J.G.V. thanks the National Science Foundation for generous support of this research in the form of a grant. The authors thank L. J. Vande Griend for assistance.

Supplementary Material Available: A listing of structure factor amplitudes (5 pages). Ordering information is given on any current masthead page.

References and Notes

- (1) Camille and Henry Dreyfus Foundation and Teacher-Scholar Grant Awardee, 1972-1977 and Fellow of the Alfred P. Sloan Foundation, 1973-1975.
- (2) D. W. White and J. G. Verkade, *Phosphorus*, **3**, 9 (1973).
- (3) (a) L. J. Vande Griend and J. G. Verkade, *Phosphorus*, **3**, 13 (1973); (b) L. J. Vande Griend, J. G. Verkade, J. F. M. Pennings, and H. M. Buck, submitted.
- (4) L. J. Vande Griend, D. W. White, and J. G. Verkade, *Phosphorus*, **3**, 5 (1973).
- (5) (a) J. G. Verkade, *Coord. Chem. Rev.*, **9**, 1 (1972); (b) L. J. Vande Griend and J. G. Verkade, to be submitted for publication.
- (6) J. O. Albright, F. L. Tanzella, and J. G. Verkade, *J. Coord. Chem.*, in press.
- (7) J. G. Verkade, *Bioinorg. Chem.*, **3**, 165 (1974).
- (8) (a) J. G. Verkade, Plenary Lecture, Vth International Conference on Organic Phosphorus Chemistry, Gdansk, Poland, Sept 1975; *Phosphorus*, in press;
- (b) R. F. Hudson and J. G. Verkade, *Tetrahedron Lett.*, 3231 (1975); (c) J. A. Mosbo and J. G. Verkade, *J. Am. Chem. Soc.*, **95**, 4659 (1973); (d) W. G. Benitude, H. W. Tan, and K. C. Yee, *J. Am. Chem. Soc.*, **97**, 573 (1975).
- (9) J. E. Casida, M. Eto, A. D. Mosconi, J. L. Engel, D. S. Milbrath, and J. G. Verkade, *Toxicol. Appl. Pharmacol.*, in press.
- (10) M. G. Newton and B. S. Campbell, *J. Am. Chem. Soc.*, **96**, 7790 (1974).
- (11) L. S. Khaikin and L. V. Vilkov, *J. Struct. Chem. (Engl. Transl.)*, **10**, 614 (1969).
- (12) S. Wawzonek, A. Matar, and C. H. Issidorides, *Org. Synth.*, **38**, 68 (1958).
- (13) C. W. Heltsch and J. G. Verkade, *Inorg. Chem.*, **1**, 392 (1962).
- (14) G. Germain, P. Main, and M. M. Woolfson, *Acta Crystallogr., Sect. B*, **24**, 274 (1970).
- (15) W. R. Busing, K. O. Martin, and H. A. Levy, "OR FLS, A Fortran Crystallographic Least Squares Program", U.S. Atomic Energy Commission Report ORNL-TM-305, Oak Ridge National Laboratory, Oak Ridge, Tenn., 1962.
- (16) C. R. Hubbard, C. O. Quicksall, and R. A. Jacobson, "The Fast Fourier Algorithm and the Programs ALFF, ALFDP, ALFFPROJ, ALFFT, and FRIEDEL", U.S. Atomic Energy Commission Report IS-2625, Iowa State University and Institute for Atomic Research, Ames, Iowa, 1971.
- (17) C. K. Johnson, "OR TEP-II: A Fortran Thermal-Ellipsoid Plot Program for Crystal Structure Illustrations", U.S. Atomic Energy Commission Report ORNL-3794, (2d Revision with Supplemental Instructions, Oak Ridge National Laboratory, Oak Ridge, Tenn., 1970. All drawings depict 30% probability ellipsoids.
- (18) See paragraph at the end of this paper concerning supplementary material.
- (19) H. P. Hanson, F. Herman, J. D. Lea, and S. Skillman, *Acta Crystallogr.*, **17**, 1040 (1964).
- (20) "International Tables for X-Ray Crystallography", Vol. III, 2d ed, Kynoch Press, Birmingham, England, 1962, pp 214-216.
- (21) The endocyclic OPO angle of 95.1° undoubtedly reflects the presence of strain in the five-membered ring of 3.¹⁰
- (22) J.-M. Lehn and G. Wipff, *J. Chem. Soc., Chem. Commun.*, 800 (1975).
- (23) D. M. Nimrod, D. R. Fitzwater, and J. G. Verkade, *J. Am. Chem. Soc.*, **90**, 2780 (1968).
- (24) D. E. C. Corbridge, *Top. Phosphorus Chem.*, **3**, 57 (1966).

Structure and Conformation of Cyclo(tri-L-prolyl) in the Crystalline State

Mary Ellen Druyan,*^{1a} Charles L. Coulter,*^{1b} Roderich Walter,^{1c} G. Kartha,^{1d} and G. K. Ambady^{1d}

Contribution from the Department of Anatomy, University of Chicago, Chicago, Illinois 60637, and the Hines V.A. Hospital, Hines, Illinois 60141.

Received January 23, 1976

Abstract: Cyclo(tri-L-prolyl), C₁₅H₂₁O₃N₃, is made up of three prolyl residues joined by cis peptide bonds. A single-crystal x-ray diffraction study of the compound has been done. The crystals are orthorhombic, space group *P*2₁2₁2₁ with *a* = 15.942 (5), *b* = 19.097 (6), and *c* = 9.230 (3) Å and *Z* = 8. Intensity data were collected on a diffractometer using Mo x-radiation, and absorption corrections were made. The final *R* value for the 3167 data was 4.8%. In the peptides for the two molecules in the asymmetric unit, the N and its substituents show deviations from planarity, and the bond angles about N are different from those found in other prolyl residues. Two of the six prolyl rings have a C_α-envelope conformation, and the other four rings a C_α-C_β twist conformation. The conformations are closely related, and the barriers between them in solution must be small in order to explain the equivalence of the three C_α-protons in the proton magnetic resonance spectrum of cyclo(tri-L-prolyl). One of the H_α-C_α-C_β-H_β torsion angles is 90° in all six prolyl rings, but the other torsion angles show considerable variation. The packing involves several close oxygen to methylene carbon contacts.

The role of structural determinants such as amino acid sequence and chemical environment in overall peptide or protein conformation is a continuing interest of both theoreticians and experimentalists.^{2,3} Proline residues in proteins and oligopeptides impart particular restraints on the conformational freedom of nearby peptide units, and, in turn, the degree of conformational flexibility of the proline residue is related to the overall polypeptide conformation. Cyclic peptides containing proline residues are of particular structural interest because the cyclization usually imposes additional conformational constraints.^{4,5} There have been a number of crystallographic investigations of proline and proline-containing

molecules,⁶⁻¹⁹ and structural information from these studies and from NMR studies^{5,20-25} has been related to prolyl ring conformation and used in conformational energy analyses.⁴ Early model building studies of proline-containing peptides treated the pyrrolidine ring as either planar or puckered, but in all cases rigidity of the ring was assumed. Current experimental and theoretical evidence suggests that there is variability in the puckering of the prolyl ring, and that flexibility of the ring must be considered along with the effects of ring geometry on the backbone conformation.

Cyclo(tri-L-prolyl), which was first synthesized by Rothe et al.,²⁶ is unusual among peptides in its restricted conforma-